FULL PAPER

ADVANCED FUNCTIONAL MATERIALS

Bifunctional Carbon Nanotubes by Sidewall Protection**

By *Nitin Chopra*, *Mainak Majumder*, and *Bruce J. Hinds**

A vertically aligned array of multiwalled carbon nanotubes (MWCNTs) impregnated with polystyrene is utilized to independently functionalize each end of the MWCNTs. The presence of the polystyrene matrix prevents sidewall oxidation of the CNTs, resulting in carboxylate derivatization at the CNT tips during processing via plasma oxidation. The membrane is subsequently dissolved in toluene, resulting in a suspension of CNTs with carboxylate-derivatized tips. The CNT tips are further functionalized using carbodiimide-mediated linking of carboxylate at the CNT tips with an amine of 2-aminoethanethiol. This treatment results in thiol functionality and Fourier-transform infrared (FT-IR) studies confirm amide-bond formation. Gold nanoparticles that are readily observed using transmisison electron microscopy (TEM) are then covalently linked to the thiol functional groups. Estimates of the average nanoparticle density are observed to decrease from ~526 particles μm^{-1} near the CNT tips to negligible values (< 7 particles μm^{-1}) at locations beyond 700 nm from the CNT tips. This is consistent with a membrane geometry where CNTs tips are above the polystyrene surface owing to differing oxidation rates. Bifunctional CNTs (with different chemical functionality at either end of each CNT) is achieved by thiol functionalization on only one side of the oxidized CNT membrane floating on top of a 2-aminoethanethiol functionalization reaction solution. After dissolution of the polystyrene matrix, TEM analysis shows gold-nanoparticle decoration at the thiol-functionalized end of the CNT.

1. Introduction

Carbon nanotubes (CNTs) are functional materials with unique chemical, electrical, and mechanical properties. There are numerous reports demonstrating the ability to chemically functionalize CNTs for biological applications.[1–4] Such chemistry is readily transferable to numerous applications such as sensors,[5,6] electrodes for oxidation,[7] fuel cells,[8] electronic devices and interconnects,[9–11] and heterogeneous catalysis.[12] Another novel application of CNTs is to use them as shadow masks[13,14] resulting in nanometer-scale lines during line-of-site deposition processes. Such applications require control of diameter and selective placement of CNTs. Thus, a reliable means to self-assemble nanotubes onto substrates can result in more efficient and better controlled nanometer-scale lithography processes. CNTs are chemically stable and highly hydrophobic in nature. Therefore, they require surface modification in order to establish effective CNT–substrate interactions.[15] There are various examples of sidewall functionalization, including coating with a polymer, surfactant, or DNA, resulting in uniform dispersion or separation of CNTs.[16–19] In addition, oxidation of CNTs can result in tip and sidewall derivatization with phenolic and carboxylic groups which can be further linked to a variety of molecules,[20] such as thiols, amines,[21] or thionyl chloride.[22] When functionalized, a CNT can be covalently[23] or electrostatically[24] linked to other nanostructures including the CNT itself.[25] However, a common problem is functionalization along the CNT sidewalls which results in unwanted reactive sites. The process of CNT functionalization is inherently indiscriminant, as seen in reports of CNTs coated with ZnS[26] and Au[27–29] nanoparticles. These functionalization methods involve chemical oxidation processes which not only oxidize the entire CNT area, but also uncontrollably cut the length of the CNTs. For many CNT applications, such as directed self-assembly, it is required that there be well-controlled functionalization chemistry at the CNT tips only. Fortunately, oxidation processes can result in a high concentration of carboxyl groups at the tips that are readily tailored by elementary carbodiimide chemistry. Carboxyl groups (–COOH) can be derivatized with thiol terminal groups, such as NH_2–$(CH_2)_{11}$–SH. Then, the CNTs can be decorated with gold nanoparticles to readily show the spatial location of chemical functionalization.[30] However, the selective functionalization of CNT tips without sidewall functionalization remains a major challenge.

Template-assisted growth of nanowires, followed by functionalization at nanowire tips and removal of the membrane matrix, has demonstrated an ability to selectively functionalize nanowire tips.[31] Recently a multiwalled CNT (MWCNT)-based membrane structure was fabricated by impregnating an aligned CNT array with a polystyrene film by a simple spin-coating process.[32] A water (H_2O) plasma-oxidation process opens the CNT tips (normally blocked with catalytic Fe nano-

[*] Dr. B. J. Hinds, N. Chopra, M. Majumder
Department of Chemical and Materials Engineering
University of Kentucky
Lexington, KY 40506 (USA)
E-mail: bjhinds@engr.uky.edu
Dr. B. J. Hinds
Department of Chemistry, University of Kentucky
Lexington, KY 40506 (USA)

[**] The authors thank Rodney Andrews and Dali Qian the Center for Applied Energy Research (Univ. of KY) for supplying MWCNTs. The Center for Micro-Magnetic Electronic Devices and Electron Microscopy Center at Univ. of Kentucky provided critical equipment infrastructure. Sponsorship was provided by Air Force Office of Scientific Research (DEPSCoR program) under agreement #F49620-02-1-0225 and NSF CAREER award (CTS-0348544).

  DOI: 10.1002/adfm.200400399

ADVANCED FUNCTIONAL MATERIALS

crystals) and oxidized CNT tips were exposed on both sides of membrane. Importantly this oxidative chemistry affects only the tips of the CNTs, since the CNT sidewalls are protected by the polystyrene matrix. These tips can be further derivatized by simple carbodiimide chemistry. In fact, it should be possible to derivatize each side of the membrane differently by floating the membrane on top of different reaction solutions.

2. Results and Discussion

To selectively functionalize CNT ends we used aligned MWCNT membranes as our source of CNTs, using a previously described method.[32] Briefly, an aligned array of MWCNTs was grown by chemical vapor deposition using ferrocene/xylene feed gas. The volume between the CNTs was filled with polystyrene and the composite film was removed from the quartz substrate. Excess surface polymer, as well as Fe nanocrystals at the CNT tips, were removed by H_2O-plasma oxidation. This resulted in MWCNTs traversing the polystyrene film with carboxylic (–COOH) group functionalization at the CNT tips. Figure 1A shows a cross-sectional scanning electron microscopy (SEM) image of ~10 μm thick aligned MWCNTs in a polystyrene matrix. Importantly for this study,

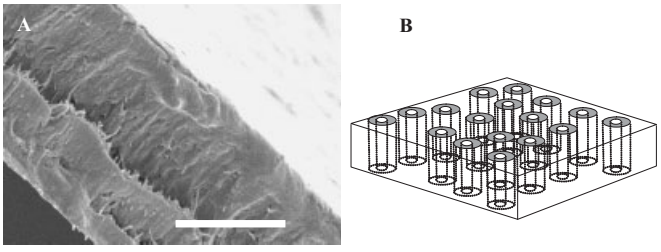

Figure 1. A) Cross-sectional SEM image (scale bar: 5 μm) of a ~10 μm thick CNT membrane. Note the CNT alignment across the polystyrene matrix. B) Schematic of MWCNTs in a polystyrene matrix after a plasma-oxidation process. Hollow cores of aligned MWCNTs pass across a continuous polymer film to form a membrane structure.

the sidewalls of the CNTs were protected from the oxidation process by the polystyrene film, resulting in the oxidation of CNTs only at their ends, as shown in Figure 1B. Furthermore, the carboxylic-derivatized CNT tips offer a wide range of possibilities for selective derivatization at the CNT tips through carbodiimide chemistry. For observing the chemistry at the CNT tips, the polystyrene–CNT composite was dissolved in toluene and rinsed several times to obtain a clean suspension of CNTs. Using 1-ethyl-3-[3-dimethyl aminopropyl]carbodiimide hydrochloride (EDC) as linker in pH 4 buffer solution and water as reaction medium, carboxylic acid-terminated CNT tips were thiol-derivatized with 2-aminoethanethiol [H_2N–$(CH_2)_2$–SH]. Chemical derivatization of suspended CNTs (without a polystyrene matrix) was confirmed by Fourier-transform infrared (FT-IR) studies, as shown in Figure 2a–c. FT-IR spectra were compared for a) CVD-grown CNTs, b) CNTs obtained after dissolution of a plasma and acid-oxidized CNT membrane, and c) 2-aminoethanethiol-functionalized CNTs. As expected, plasma oxidation resulted in an increase of carbonyl and O–H stretches. 2-Aminoethanethiol derivatization resulted in the broad C–H stretches and a shift in the location of the carbonyl peak. Of most interest are the carbonyl groups (Fig. 2B), as the as-received CVD-grown CNTs did not show a carbonyl stretch. However, in the case of plasma-oxidized CNTs obtained after membrane dissolution, a carbonyl peak was apparent at 1630 cm^{-1} (dotted line in Fig. 2A), attributed to the carboxylic acid (–COOH) group. For chemically oxidized single-walled carbon nanotubes (SWCNTs), carbonyl stretches for carboxyl groups have been found in the range 1700–1750 cm^{-1}.[33,34] It appears that due to the larger inner-core diameter (~7 nm) of MWCNTs, as compared to SWCNTs (~1–2 nm), MWCNTs have carbonyl stretches at lower frequencies (~1630 cm^{-1}). This frequency is commonly observed in planar extended aromatic systems.[35] Interference from oxidized polystyrene is not expected owing to the extensive cleaning process to dissolve the polymer film and suspend the MWCNTs. Figure 2A also shows the increase in the O–H peak intensity at 3400–3500 cm^{-1} for the plasma-oxidized CNTs and 2-aminoethanethiol-functionalized CNTs, compared to the as-received CNTs. This indicates the formation of excess hydroxyl groups, which is consistent with carboxylic and phenol groups resulting from plasma oxidation. However, H_2O absorption in a KBr pellet makes this trend difficult to quantify. Expansion of the carbonyl region (Fig. 2B and dotted lines in Fig. 2A) for the 2-aminoethanethiol-functionalized CNTs showed a shoulder at 1590 cm^{-1}, indicative of amide-bond formation. A shoulder at 1630 cm^{-1} remains, indicating that not all carbonyl groups are derivatized. Liu et. al.[36] also found similar shifts in the amide-I stretch (band at 1600 cm^{-1}) for 2-aminoethanethiol-functionalized CNTs. Peaks in the range 2800–3050 cm^{-1} (aromatic C–H stretch) (Fig. 2A) can be attributed to toluene solvent. However, it is difficult to differentiate between polystyrene and toluene as they have similar IR signatures. An attempt was made to determine sulfur in 2-aminoethanethiol-functionalized CNTs using an energy-dispersive X-ray spectroscopy (EDX) study in analytical transmission electron microscopy (TEM). Carbon deposition and the detection limit of the EDX detector (~1 %) made it difficult to detect a monolayer of 2-aminoethanethiol on the CNT tips.

FTIR studies cannot measure the spatial distribution of the functionalized groups, but are supportive methods for confirming the presence of functionalized groups on CNTs. The spatial location of functionalized groups can be observed via gold-nanoparticle decoration of thiol functional groups on the CNTs. Gold nanoparticles can be easily covalently linked to thiol-terminated molecules[37] and can be conveniently observed with electron microscopy to demonstrate the presence of the functional group.[38] Jiang et al.[27] have selectively attached gold nanoparticles to nitrogen-doped CNTs. The process involved coating CNTs with a uniform layer of polyelectrolyte that electrostatically interacts with negatively charged gold nanoparticles. In the process reported here, the functionalization and dissolution process does not involve any polyelec-

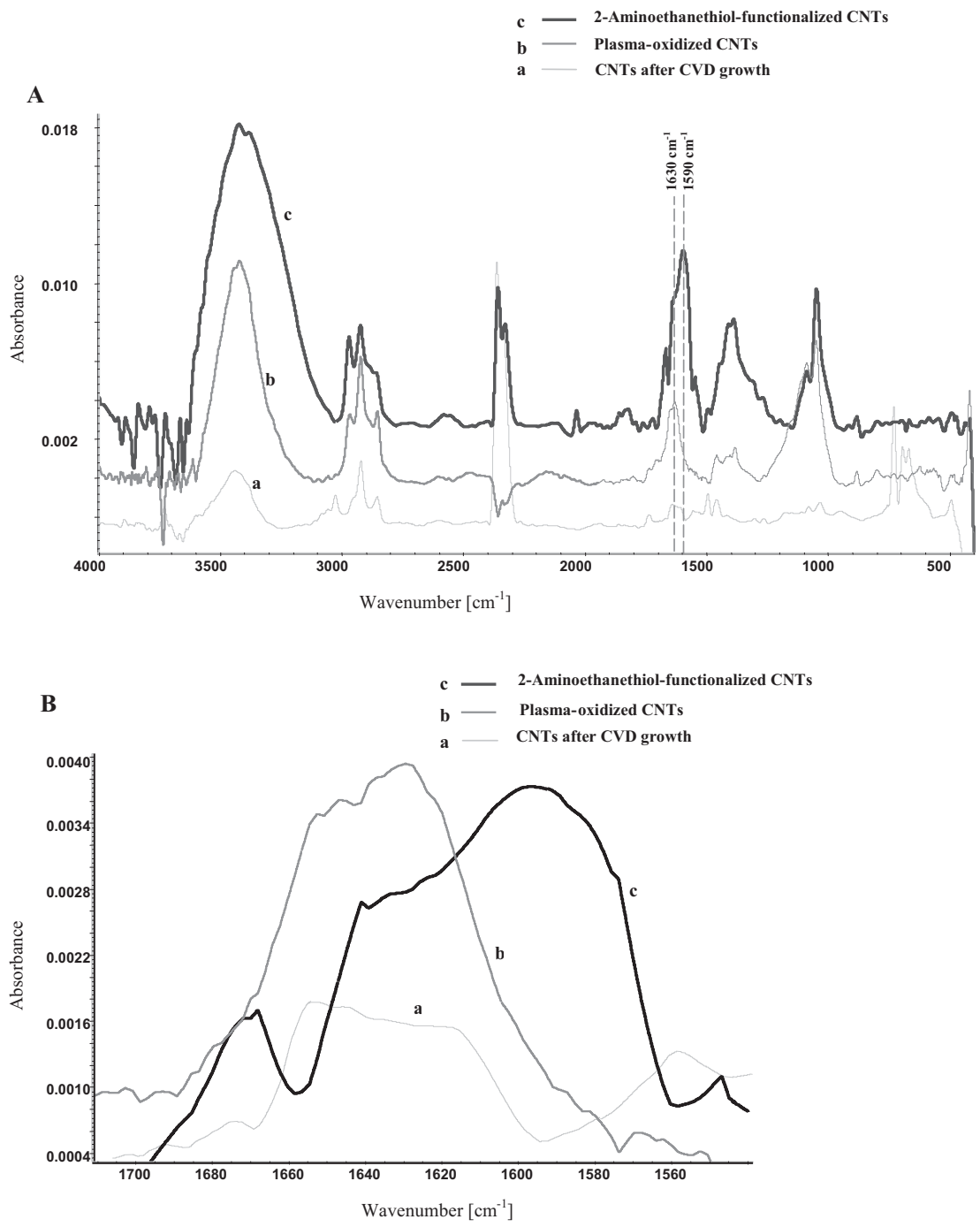

Figure 2. A). FT-IR spectra of CNTs at various stages of functionalization. Spectra are offset for clarity. Dotted arrows indicate the shift of the carbonyl peak for 2-aminoethanethiol-functionalized CNTs (1590 cm^{-1}) in plasma-oxidized CNTs (1630 cm^{-1}). B) Expanded FT-IR spectra of carbonyl-stretch region (1550–1700 cm^{-1}) at various stages of CNT functionalization. The baseline is adjusted for clarity.

trolyte, and the interaction of CNTs with gold nanoparticles is through covalent Au–S bonding. The TEM images in Figure 3 show a high-density of gold nanoparticles at the CNT tips, indicating of selective functionalization of the CNT ends. Also observed in TEM images (Fig. 3) is that the CNTs, after dissolution and cleaning processes, are free from the polymer which initially protected the CNT sidewalls from oxidation. An observable amount of sidewall functionalization can be attributed to the presence of defects created during the growth of the CNTs (ultrasonication of CNTs during cleaning and dispersion processes) or physisorption during the final rinsing step.

Aqueous-acid treatment of oxidized CNTs for creating phenolic and carboxylic groups on the CNT surface and tip resulted in end-to-end and end-to-side interconnected CNTs.[25]

ADVANCED FUNCTIONAL MATERIALS

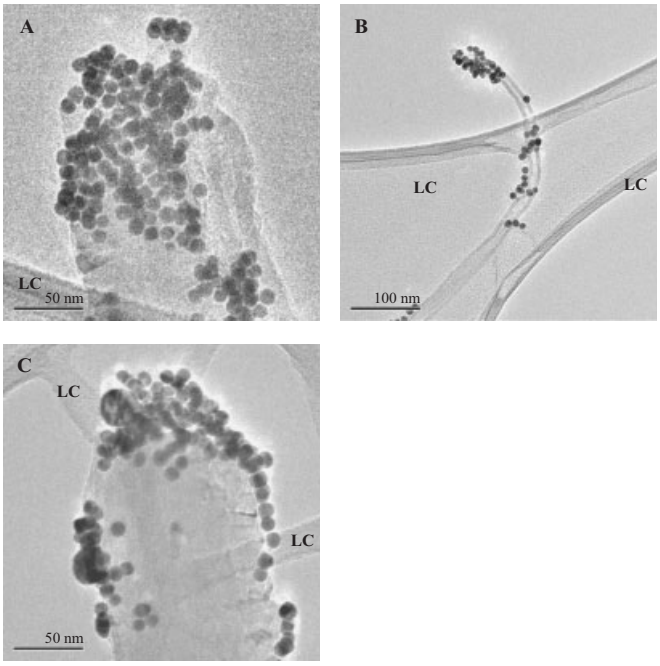

Figure 3. TEM image showing gold-nanoparticle decoration at thiol-functionalized sites on a CNT tip: A) CNT tip decorated with gold nanoparticles (scale bar: 50 nm); B) CNT tip decorated with gold nanoparticles and showing minimal sidewall functionalization (scale bar: 100 nm); and C) CNT tip decorated with gold nanoparticles showing decoration along the CNT length near the tip (scale bar: 50 nm). 'LC' indicates the edges of the lacey carbon from the TEM grid.

However, strong solution-based oxidation treatment uncontrollably attacks the CNT surface and cuts them so they are shorter. Suspensions of MWCNTs are particularly susceptible to sidewall functionalization during solution-based oxidation, since the outer layers can be oxidized without completely cutting the entire tube. Because the sidewalls are protected by polystyrene during the oxidation process, almost the original length of the CNTs (~5–10 μm), determined by the membrane thickness, is maintained.

An estimate of nanoparticle density can be obtained from TEM images by counting the number of Au nanoparticles (10 nm diameter) seen along a given length of a CNT. This observation was made for more than thirty different CNTs and the average nanoparticle density is shown in the histogram of Figure 4. The density [particles (μm length)$^{-1}$] decreases from ~526 particles μm^{-1} (in the first ~34 nm of CNT length), to negligible values (<7 particles μm^{-1}) at a location beyond 700 nm from the tip. Because polystyrene etches faster than CNTs in the plasma oxidation of membranes, the tips of the CNTs were observed to be slightly above the polymer film.[32] Therefore, a small portion of the CNT sidewall on both sides of membrane is exposed to oxidation. For an average length of 34 nm, starting from the CNT tip, the average nanoparticle coverage (ratio of total projection area of nanoparticles to total surface area of sidewall exposed to oxidation) was approximately ~20 %. The average coverage (ratio of total projection area of nanoparticles to total surface area at tips) at the CNT tips was approximately ~52 %. With 10 nm diameter nanocrystalline Au (nc-Au), the maximum functionality detectable at saturation (i.e., 100 % coverage) is 10^{12} (reactive sites) cm^{-2}. From nc-Au coverage, an estimate of surface functionality is 5×10^{11} sites cm^{-2} at the tips and 2×10^{11} sites cm^{-2} along the sidewalls of the CNTs above the polystyrene matrix. Multiple reactive sites can be under the nc-Au, so this TEM observation is a lower-limit estimate of actual thiol functionality. As a reference, the density of broken carbon bonds at the edge of cleaved graphite and density of graphitic carbon on a surface are 1.5×10^{15} and 3.5×10^{15} cm^{-2}, respectively. On average, it appears that a small percentage of all possible carbon atoms at the tips and exposed CNT sidewalls are thiol-functionalized. Since functional coverage is relatively low (several of the thiol molecules tether per nanoparticle), we do not see evidence that the nc-Au is bound strongly enough to the CNT surface to experience significant stress. However, this would be an interesting line of future research. Though ~30 nm of a MWCNT is above polystyrene matrix (thus subject to sidewall oxidation), it is possible to selectively electrochemically oxidize[39] only the conductive CNT down into the insulating polystyrene matrix.[32] This would result in selective functionalization of the etched MWCNTs only at the tips, since no CNT sidewall would be exposed above the polystyrene matrix to an oxidative solution.

Using MWCNT membranes, it is possible to functionalize only one side of a membrane by floating the membrane on top

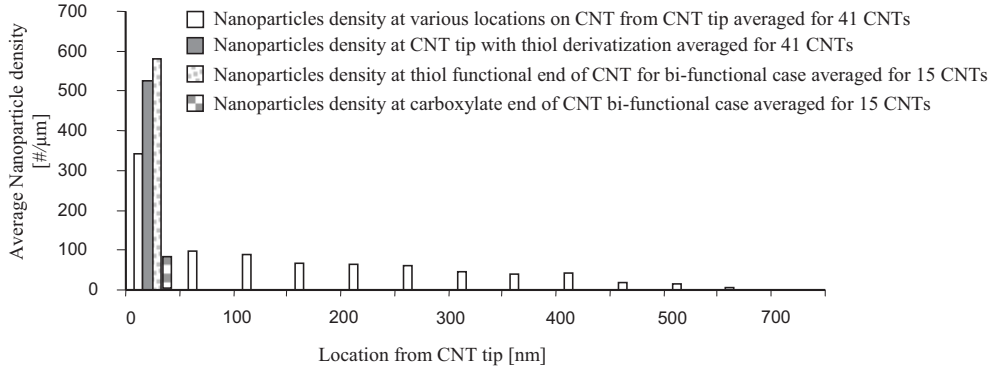

Figure 4. Histogram indicating estimates of average nanoparticle density versus distance from the CNT tip, obtained from TEM observations.

of a reactive solution of 2-aminoethanethiol and EDC linker. The hydrophobic nature of polystyrene allows sufficient surface tension to float the membrane on top of the aqueous solution. This approach, allowing exposed CNT tips on only one side of membrane to come into contact with functionalization solution, is shown in Scheme 1.

Dissolution of such membrane in toluene results in a suspension of bifunctional MWCNTs. Bifunctional in this case means that CNTs have different functional chemistry (thiol or carboxyl) at each end of the CNT. To monitor this bifunctional character, a colloidal gold-nanoparticle solution was added to an ethanolic solution of bifunctional CNTs. Gold-nanoparticle decoration occurred at the thiol-derivatized end of the CNTs, while the carboxyl end had only background amounts. This was consistently observed in TEM images shown in Figures 5A–D. Figure 4 includes the histogram of fifteen different CNTs with selective thiol or carboxylate functionality near the CNT tip. The thiol-functionalized end had an estimated nanoparticle density of ~580 μm^{-1} on an average length of ~44 nm starting from the CNT tip. The carboxyl-functionalized MWCNT end had an average nanoparticle density of ~80 nanoparticles μm^{-1}, which is the same density as for non-derivatized sidewalls. The TEM grid with a CNT-nanoparticle dispersion was washed with ethanol in a vacuum filtration process to remove unbound gold nanoparticles. However, the rinsing process was not completely effective as a few clusters of particles are seen on the lacey carbon TEM grid (Figs. 5A,C). This artifact can possibly add nc-Au to CNT sidewalls, even though there is no thiol functionality and contribute to the 'base-line' nc-Au seen at distances far from the tip.

Figure 4D also shows nanocrystalline Fe (nc-Fe) in the core of CNT, due to the higher amount of ferrocene in the CVD process. This CNT–polystyrene composite came from a region of the substrate that had a relatively high concentration of nc-Fe. Specific to this bifunctional derivatization of CNTs, chemi-

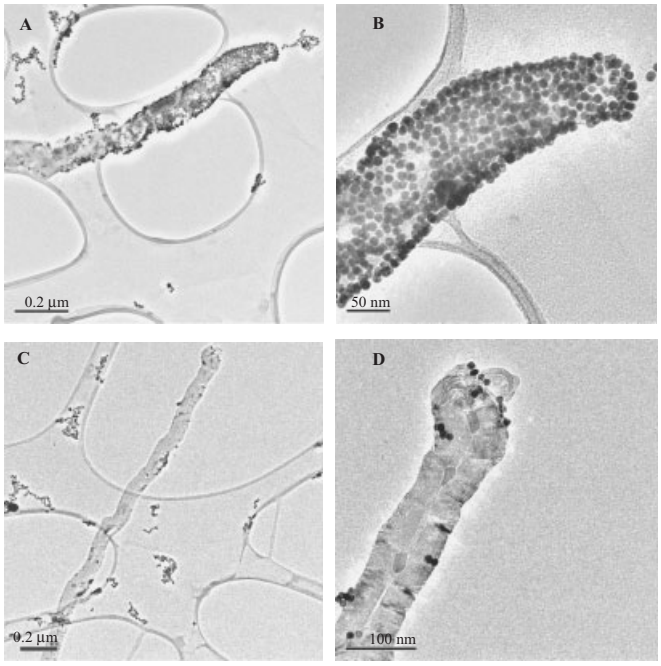

Figure 5. Bifunctionalized CNTs. A,B) Thiol-functionalized CNT with gold-nanoparticle decoration (scale bars: 0.2 μm and 50 nm, respectively). C,D) The other end of the same MWCNT with only carboxylate functionality and minimal gold decoration (scale bars: 0.2 μm and 100 nm, respectively). Note that in (A,C) some unbound gold-nanoparticle clusters are present on the lacey carbon—a result of the cleaning process.

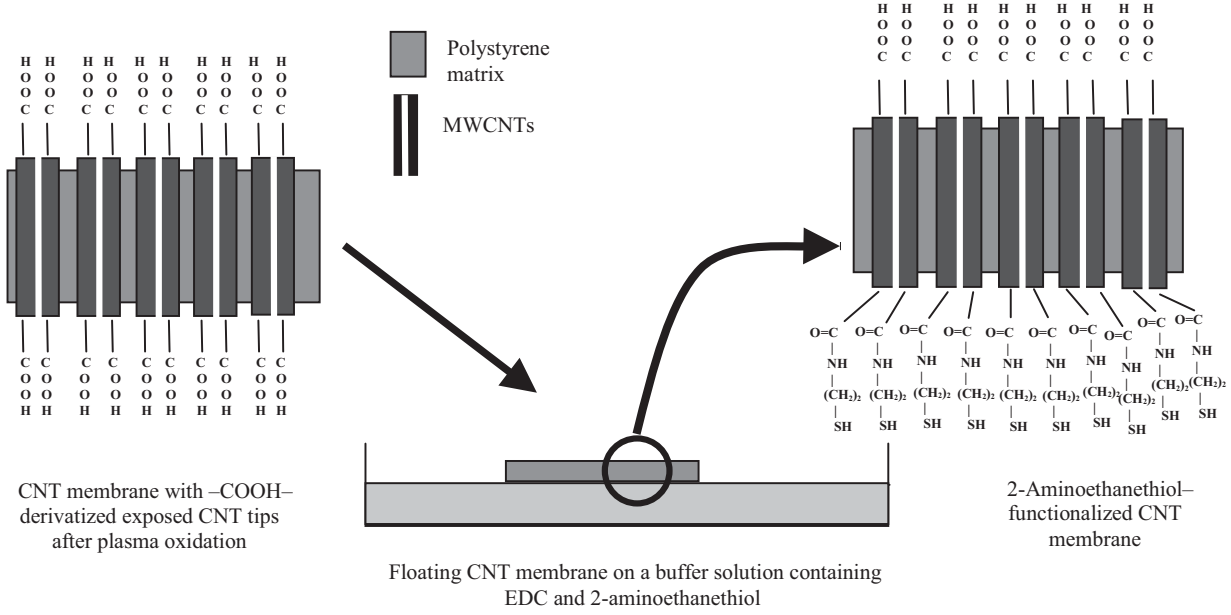

Scheme 1. Plasma-oxidized aligned CNT membrane (cross-sectional view) with carboxylic acid-derivatized CNTs when floated on a buffer solution containing EDC and 2-aminoethanethiol, resulted in bifunctional CNTs in the membrane structure.

ADVANCED FUNCTIONAL MATERIALS

cal transport across the membrane is not required. An aligned CNT–polystrene composite is preferred as a source of sidewall-protected and tip-derivatized MWCNTs. Increasing ferrocene content in the CVD process can readily accomplish this over the entire substrate area, if this is desired. It is also noteworthy to mention that the approach shown here of floating a sidewall-protected film on top of a derivatization solution can similarly be applied to template-grown nanowire systems that utilize porous alumina membranes. This is a modification of the approach that gives nanowire ends the same chemical functionalization.[31] However the hydrophilic nature of porous alumina may not allow the membrane to float but would simply require specialized reaction adaptors.

3. Conclusions

Aligned MWCNT membranes can be utilized to selectively functionalize each end of MWCNTs. During the oxidation process, CNT sidewalls are protected by a continuous polystyrene matrix, resulting in negligible sidewall functionalization. The presence of functionalized groups on CNTs was further confirmed by FTIR studies. The spatial location of thiol-derivatized CNT ends were readily observed using TEM by the covalent attachment of gold nanoparticles. Dissolution of the polystyrene matrix results in a suspension of MWCNTs with each end having a different chemical functionality. Such controlled functionalization processes can be used to create self-directed patterned architectures.

4. Experimental

Aligned MWCNT membranes were fabricated using previously reported method [32]. A 1 cm × 1 cm piece of CNT membrane was dissolved in toluene (Mallinckrodt) resulting in dark-black solution. The CNT solution was ultrasonicated and rigorously washed in toluene, acetone (Mallinckrodt), *N*,*N*-dimethylformamide (DMF, Mallinckrodt), and ethyl alcohol (Aaper Alcohol and Chemical Co.). After drying cleaned CNTs in air for 12–24 h, 3 mL of DMF was added resulting in semi-transparent, light-gray-colored solution. To perform functionalization on CNTs, ~2 mol of 2-aminoethanethiol (H_2N–$(CH_2)_2$–SH, TCI America), ~0.5 mol of 1-[3-(dimethylamino) propyl]-3-ethylcarbodiimide hydrochloride (EDC, 98%, Aldrich), and 3 mL of CNT solution (in DMF) were added to the 15 mL of pH 4 0.1 M (2-*N*-morpholino)ethanesulfonic acid (MES, 99 %, Sigma) buffer solution in distilled water (18.1 MΩ cm^{-1}, Barnstead). The solution was stirred vigorously for 3–4 days and then centrifuged at 3400 rpm (rpm: revolutions per minute) for 30 min and the supernatant removed. The remaining black residue was washed with acetone, water, ethyl alcohol, and dried in air for 4–5 h. 3 mL of ethyl alcohol and 2 mL of concentrated gold-nanoparticle solution (10 nm diameter, Sigma) was added to the dried CNTs and the solution was vigorously stirred for 24 h.

To prepare CNTs with only one end having thiol functionalization, ~2 mol of 2-aminoethanethiol, ~0.5 mol of EDC, and 3 mL of CNT solution (in DMF) was added to 30 mL of pH 4, 0.1 M MES buffer solution in DI water. The solution was slowly stirred and a 0.8 cm × 0.5 cm piece of CNT membrane was gently floated on the solution surface. The reaction was allowed to occur for 3–4 days, after which the membrane was taken out and washed in water for 3–4 h. A dried piece of membrane was dissolved in toluene and centrifuged at 3400 rpm for 30 min and ultrasonicated in toluene, acetone, and ethyl alcohol. The supernatant was discarded each time and finally the black residue left was dried in air for 24 h. 2 mL of concentrated gold-nanoparticle solution was added to 5 mL of CNT solution in ethyl alcohol and stirred vigorously for 24 h.

A few drops of resultant CNT–gold nanoparticle solution from each experiment were dispersed on two separate lacey carbon TEM grids (300 mesh Cu lacey carbon, SPI supplies). To further remove any remaining polystyrene and unbound gold nanoparticles, each grid was rinsed with ethyl alcohol in a vacuum-filtration setup using a polytetrafluoroethylene (PTFE) filter membrane (0.2 μm pore size, Cole-Parmer). The grids were finally dried in an oven at 40 °C for 24 h before TEM characterization using a JEOL 2010 F HRTEM. The images were acquired at 200 keV of incident electron voltage.

FT-IR spectroscopy was performed to identify functional groups in CVD-grown CNTs, plasma-oxidized CNTs, and 2-aminoethanethiol-functionalized CNTs. A small portion 2-aminoethanethiol-functionalized CNT membrane is dispersed (after dissolution, centrifuge separation and rinsing) in a solution of toluene and then mixed with FT-IR-grade KBr (powder > 99 %, Sigma). 2.5 mg of plasma-oxidized and-acid treated CNT membrane was dissolved in 5 gm of toluene, ultrasonicated for 5–10 min, and then centrifuged 4–5 times to remove the dissolved polymer. The purified nanotubes in toluene were then mixed with FT-IR-grade KBr. As-received and CVD-grown CNTs on a quartz substrate were removed and mixed with KBr in toluene. All three CNT–KBr mixtures were dried in a vacuum oven (Precision) for 12 h at 120 torr pressure. The dried powder was then examined in ThermoNicolet Nexus 4700 FT-IR instrument. An FT-IR spectrum of KBr was also taken for subtraction and correction purposes.

Received: September 15, 2004
Final version: November 5, 2004

[1] S. E. Baker, W. Cai, T. L. Lasseter, K. P. Weidkamp, R. J. Hamers, *Nano Lett*. **2002**, *2*, 1413.
[2] C. Dwyer, M. Guthold, M. Falvo, S. Washburn, R. Superfine, D. Erie, *Nanotechnology* **2002**, *13*, 601.
[3] C. V. Nguyen, L. Delzeit, A. M. Cassell, J. Li, J. Han, M. Meyyapan, *Nano Lett.* **2002**, 2, 1079.
[4] S. Wang, E. S. Humphreys, S. Y. Chung, D. F. Delduco, S. R. Lustig, H. Wang, K. N. Parker, N. W. Rizzo, S. Subramony, Y. M. Chiang, A. Jagota, *Nat. Mater*. **2003**, 2, 196.
[5] S. Hrapovic, Y. Liu, K. B. Male, J. H. T. Luong, *Anal. Chem*. **2004**, *76*, 1083.
[6] Y. Lu, J. Li, J. Han, H. T. Ng, C. Binder, C. Patridge, M. Meyyapan, *Chem. Phys. Lett*. **2004**, *391*, 344.
[7] P. J. Britto, K. S. V. Santhanam, P. M. Ajayan, *Bioelectrochem. Bioenerg*. **1996**, *41*, 121.
[8] X. Sun, R. Li, D. Villers, J. P. Dodelet, S. Desilets, *Chem. Phys. Lett*. **2003**, *379*, 99.
[9] Y. Homma, T. Yamashita, Y. Kobayashi, T. Ogino, *Physica B* **2002**, *323*, 122.
[10] F. Kreupl, A. P. Graham, G. S. Duesberg, W. Steinhogl, M. Liebau, E. Unger, W. Honlein, *Microelectron. Eng.* **2002**, *64*, 399.
[11] S. Ravindran, S. Chaudhary, B. Colburn, M. Ozkan, C. S. Ozkan, *Nano Lett.* **2003**, *3*, 447.
[12] G. L. Che, B. B. Lakshmi, C. R. Martin, E. R. Fischer, *Langmuir* **1999**, *15*, 750.
[13] N. Chopra, R. Andrews, W. Xu, L. Delong, B. J. Hinds, *Mater. Res. Soc. Symp. Proc.* **2004**, *EXS-2*, M5.4.1.
[14] J. Lefebvre, M. Radosavljevic, A. T. Johnson, *Appl. Phys. Lett.* **2000**, *76*, 3828.
[15] T. Seeger, T. Kohler, T. Frauenheim, N. Grobert, M. Ruhle, M. Terrones, G. Seifert, *Chem. Comm.* **2002**, *1*, 34.
[16] Y. P. Sun, W. Huang, Y. Lin, K. Fu, A. Kitaygorodskiy, L. A. Riddle, Y. J. Yu, D. L. Carroll, *Chem. Mater.* **2001**, *13*, 2864.
[17] W. Huang, Y. Lin, S. Tayler, J. Gaillard, A. M. Rao, Y. P. Sun, *Nano Lett.* **2002**, *2*, 231.
[18] M. Shim, W. S. K. Kam, R. J. Chen, Y. Li, H. Dai, *Nano Lett.* **2002**, *2*, 285.
[19] M. Zheng, A. Jagota, E. D. Semke, B. A. Diner, R. S. Mclean, S. R. Lustig, R. E. Richardson, N. G. Tassi, *Nat. Mater.* **2003**, *2*, 338.

[20] Y. P. Sun, K. Fu, Y. Lin, W. Huang, *Acc. Chem. Res.* **2002**, *35*, 1096.
[21] S. S. Wong, E. Joselevich, A. T. Wooley, C. L. Cheung, C. M. Lieber, *Nature* **1998**, *394*, 52.
[22] J. Chen, M. A. Hamon, H. Hu, Y. Chen, A. M. Rao, P. C. Eklund, R. C. Haddon, *Science* **1998**, *282*, 95.
[23] S. Banerjee, S. S. Wong, *Nano Lett.* **2002**, *2*, 195.
[24] J. Sun, M. Iwasa, L. Gao, Q. Zhang, *Carbon* **2004**, *42*, 895.
[25] P. W. Chiu, G. S. Duesberg, U. D. Weglikowska, S. Roth, *Appl. Phys. Lett.* **2002**, *80*, 3 811.
[26] L. Zhao, L. Gao, *J. Mater. Chem.* **2004**, *14*, 1 001.
[27] K. Jiang, A. Eitan, L. S. Schadler, P. M. Ajayan, R. W. Siegal, N. Grobert, M. Mayne, M. Reyes-Reyes, H. Terrones, M. Terrones, *Nano Lett.* **2003**, *3*, 275.
[28] L. Liu, T. Wang, J. Li, Z. X. Guo, L. Dai, D. Zhang, D. Zhu, *Chem. Phys. Lett.* **2003**, *367*,747.
[29] E. Unger, G. S. Duesberg, M. Liebau, A. P. Graham, R. Seidel, F. Kreupl, W. Hoenlein, *Appl. Phys. A.* **2003**, *77*, 735.
[30] J. Liu, A. G. Rinzler, H. Dai, J. H. Hafner, R. K. Bradley, P. J. Boul, A. Lu, T. Iverson, K. Shelimov, C. B. Huffman, F. R. Macias, Y. S. Shon, T. R. Lee, D. T. Colbert, R. E. Smalley, *Science* **1998**, *280*, 1253.
[31] N. I. Kovtyukhova, T. E. Mallouk, *Chem. Eur. J.* **2002**, *8*, 4354.
[32] B. J. Hinds, N. Chopra, T. Rantell, R. Andrews, V. Gavalas, L. G. Bachas, *Science* **2004**, *303*, 62.
[33] E. Basuik, A. V. Basuik, J. G. Banuelos, J. M. Saniger-Blesa, V. A. Pokrovskiy, Y. Gromovoy, A. V. Mischanchuk, B. G. Mischanchuk, *J. Phys. Chem. B* **2002**, *106*, 1588.
[34] N. I. Kovtyukhova, T. E. Mallouk, L. Pan, E. C. Dickey, *J. Am. Chem. Soc.* **2003**, *125*, 9761.
[35] D. L. Pavia, G. M. Lampman, S. G. Kriz, *Introduction to Organic Laboratory Techniques—A Contemporary Approach*, 2nd ed., Saunders College Publishing, Philadelphia, PA **1988**.
[36] Z. Liu, Z. Shen, T. Zhu, S. Hou, L. Ying, Z. Shi, Z. Gu, *Langmuir* **2000**, *16*, 3569.
[37] S. Y. Lin, Y. T. Tsai, C. C. Chen, C. M. Lin, C. H. Chen, *J. Phys. Chem. B* **2004**, *108*, 2134.
[38] M. J. Moghaddam, S. Taylor, M. Gao, S. Huang, L. Dai, M. J. McCall, *Nano Lett.* **2004**, *4*, 89.
[39] T. Ito, L. Sun, R. M. Crooks, *Electrochem. Solid State Lett.* **2003**, *6*, C4.

